88. Metal Complexes with Macrocyclic Ligands

Part XLII[1])

Tetraazamacrocyclic Nickel(II) Complexes with a Methylthio or a Methoxy Pendant Chain as Model for Cofactor F430

by **Claudio L. Schmid, Christian Kempf, Andreas Taubert, Markus Neuburger, Margareta Zehnder,** and **Thomas A. Kaden***

Institute of Inorganic Chemistry, Spitalstrasse 51, CH–4056 Basel

and **Krzysztof Bujno** and **Renata Bilewicz**

Department of Chemistry, University Warsaw, ul. Pasteura 1, PL–02-093 Warsaw

(5.III.96)

The 14-membered macrocyclic Ni^{2+} complexes of **1** and **2**, with a methylthio pendant chain, and those of **3** and **4**, with a methoxy pendant chain, have been synthesized and their chemistry has been studied. Solution spectra in H_2O, MeCN, and DMF indicate no participation of the side-chain donor group in metal coordination. This is also the case in the solid state as shown by the X-ray structures of the Ni^{2+} complexes with **1** and **2**, in which a tetrahedrally distorted square-planar geometry around the Ni^{2+} results by the coordination of the four N-atoms of the macrocycle. Cyclic voltammetry of these complexes in MeCN reveals that Ni^{2+} is reversibly reduced to Ni^{+} between −0.7 and −0.8 V *vs.* SCE. For the complexes with **1** and **2**, the thioether bond is cleaved at more negative potentials, whereby a thiol group is formed. This thiol group is then oxidized at *ca.* +0.7 V *vs.* SCE, when a glassy C electrode is used, or at *ca.* 0 V *vs.* SCE at a dropping Hg electrode. No cleavage of the ether bond in the complexes with **3** and **4** is observed under similar conditions. Reduction of the Ni^{2+} complexes of **1** and **2** with Na-amalgam in DMF produces small amounts of methane only in the case of **1**, indicating the importance of the proximity between the Ni^{I} centre and the MeS group.

Introduction. – Methanogenic bacteria are able to reduce CO_2 to methane in a complex catabolic pathway [2]. The last step of this process is the reductive cleavage of the methylthio group in methyl-coenzyme-M by methyl-coenzyme-M-reductase, whereby F430, a hydrocorphinoid nickel macrocycle, is used as cofactor. The elucidation of the structure of cofactor F430 has revealed several interesting aspects [3]. Coenzyme F430 is the first Ni-containing tetrapyrrole with a biological function, and the coordination chemistry of this metal ion is, therefore, especially interesting. The Ni-atom is tetracoordinated by the pyrazol N-atoms, but easily binds additional axial ligands, thereby changing its electronic configuration from low-spin to high-spin [4]. The stability constants for the coordination of axial ligands have been measured and indicate that penta- as well as hexacoordinate species are formed.

The reduction of F430 to a Ni^{I} species has been achieved either electrochemically or by chemical means [5] [6]. The EPR study of the so formed Ni^{+} complex reveals that the

[1]) Part XLI: [1].

species has $S = ½$, and its EPR spectrum closely resembles EPR spectra obtained for synthetic macrocyclic Ni^+ complexes. The redox potential in THF, DMF, or MeCN is −0.89 V *vs.* SCE [6] and is close to the end of the range of potentials considered to be reachable under physiological conditions. Because of the similarity of F430 with macrocyclic complexes, $[Ni(tmc)]^{2+}$ (tmc = 1,4,8,11-tetramethyl-1,4,8,11-tetraazacyclotetradecane) was used as model to study the mechanism of methyl transfer [7].

In continuation of such ideas, we have now prepared compounds **1** and **2** in which the methylthio groups has been appended to the macrocycle, so that the stereochemistry of the reactive centres, the metal ion and the MeS group, can be controlled. For comparative purposes, we also synthesized the analogous compounds **3** and **4**, in which a methoxy group is present.

Scheme

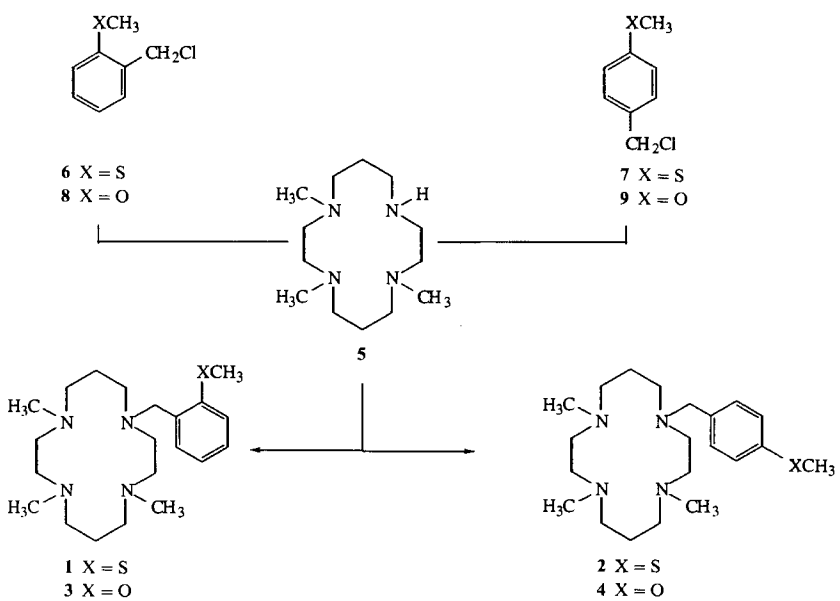

Experimental. – *General.* Compounds 1,4,8-trimethyl-1,4,8,11-tetraazacyclotedradecane (**5**) [8], 2-(methylthio)benzyl chloride (**6**) [9], 4-(methylthio)benzyl chloride (**7**) [10], 2-methoxybenzyl chloride (**8**) [11], and 4-methoxybenzyl chloride (**9**) [10] were prepared according to the literature. UV/VIS: *Perkin-Elmer Lambda 9*, 0.8 mM solns. of the complexes in H_2O, MeCN, or DMF (*Merck, Uvasol*) in 1-cm cells. IR Spectra: *Perkin-Elmer-1600* spectrophotometer, KBr pellets. ^1H- and ^{13}C-NMR Spectra: *Varian-Gemini-300* or *-400* instrument; δ rel. to $SiMe_4$ as internal standard ($\delta = 0$). GC/MS: *Hewlett-Packard* (mass selective director *5971* series, gas chromatograph *5890* series *II*, column *HP-1, SE-30*, 25 m). MS: *VG 70-250*, FAB. Elemental analyses were performed in the analytical laboratory of *Ciba AG*, Basel.

General Alkylation Procedure. To a mixture of **5** (8.26 mmol) in abs. MeCN (20 ml) and K_2CO_3 (16.53 mmol; finely pulverized and dried for 1 h at 100°), benzyl chloride **6**, **7**, **8**, or **9** (8.26 mmol) in abs. MeCN (10 ml) was added dropwise under N_2. The soln. was stirred for 3 h at r.t. and then refluxed for 3 h. K_2CO_3 was removed by filtration, the soln. evaporated, and the resulting oil dried under high vacuum and purified by FC ($MeOH/NH_3$ soln. (25%) 10:1).

1,4,8-Trimethyl-11-[2-(methylthio)benzyl]-1,4,8,11-tetraazacyclotetradecane (**1**): Yield 31%. ^{1}H-NMR ((D$_6$)DMSO): 1.50–1.59 (*quint.*, $CH_2CH_2CH_2$); 2.01, 2.11, 2.14 (3*s*, MeN); 2.35–2.56 (*m*, CH_2N); 2.42 (*s*, MeS); 3.50 (*s*, $PhCH_2N$); 7.10–7.56 (*m*, arom. H). ^{13}C-NMR ((D$_6$)DMSO): 15.44 (MeS); 24.35, 24.42 ($CH_2CH_2CH_2$); 42.67, 43.14, 43.25 (MeN); 51.30, 51.41, 53.72, 54.58, 54.82, 54.87, 55.08, 55.29, 56.57 (CH_2N); 124.56, 125.34, 127.68, 129.39, 137.00, 137.94 (arom. C). MS: 378 (M^+).

1,4,8-Trimethyl-11-[4-(methylthio)benzyl]-1,4,8,11-tetraazacyclotetradecane (**2**): Yield 40%. ^{1}H-NMR ((D$_6$)DMSO): 1.48–1.62 (*quint.*, $CH_2CH_2CH_2$); 2.03, 2.11, 2.13 (3*s*, MeN); 2.30–2.60 (*m*, CH_2N); 2.41 (*s*, MeS); 3.45 (*s*, $PhCH_2N$); 7.15–7.30 (*2d*, arom. H). ^{13}C-NMR ((D$_6$)DMSO): 14.82 (MeS); 23.87, 23.93 ($CH_2CH_2CH_2$); 42.41, 42.78, 42.87 (MeN); 50.36, 50.76, 53.43, 54.04, 54.24, 54.48, 57.69 (CH_2N); 125.69, 129.17, 135.83, 136.49 (arom. C). MS: 378 (M^+).

1-(2-Methoxybenzyl)-4,8,11-trimethyl-1,4,8,11-tetraazacyclotetradecane (**3**): Yield 34%. ^{1}H-NMR ($CDCl_3$): 1.60–1.72 (*quint.*, $CH_2CH_2CH_2$); 2.13, 2.20, 2.24 (3*s*, MeN); 2.40–2.60 (*m*, CH_2N); 3.57 (*s*, $PhCH_2N$); 3.81 (*s*, MeO); 6.82–7.20 (*m*, arom. H). ^{13}C-NMR ($CDCl_3$): 24.48 ($CH_2CH_2CH_2$); 43.14, 43.57, 43.62 (MeN); 51.32, 51.42, 52.56, 53.90, 54.12, 54.25, 54.64, 54.81, 54.89 (CH_2N); 55.30 (MeO); 110.12, 120.28, 127.49, 128.02, 130.23, 157.66 (arom. C). MS: 362 (M^+).

1-(4-Methoxybenzyl)-4,8,11-trimethyl-1,4,8,11-tetraazacyclotetradecane (**4**): Yield 32%. ^{1}H-NMR ($CDCl_3$): 1.62–1.70 (*quint.*, $CH_2CH_2CH_2$); 2.14, 2.21, 2.24 (3*s*, MeN); 2.40–2.60 (*m*, CH_2N); 3.47 (*s*, $PhCH_2N$); 3.80 (*s*, MeO); 6.81–7.26 (*2d*, arom. H). ^{13}C-NMR ($CDCl_3$): 24.35, 24.42 ($CH_2CH_2CH_2$); 43.11, 43.59, 43.62 (MeN); 50.85, 53.92, 54.17, 54.72, 54.83, 55.26 (CH_2N); 58.55 (MeO); 113.45, 130.08, 131.79, 158.48 (arom. C). MS: 362 (M^+).

General Complexation Procedure. To a soln. of the ligand **1**, **2**, **3**, or **4** (0.89 mmol) in abs. EtOH (20 ml), $Ni(ClO_4)_2 \cdot 6\,H_2O$ (0.99 mmol) was added. The soln. was refluxed during 30 min and then stirred overnight. The complex was collected by filtration, washed with abs. EtOH (4×) and Et_2O (4×), and finally dried in the dessicator.

{1,4,8-Trimethyl-11-[2-(methylthio)benzyl]-1,4,8,11-tetraazacyclotetradecane}nickel(II) Diperchlorate: Yield 95%. IR: 3420*m*, 2924*m*, 2017*w*, 1598*m*, 1474*m*, 1407*w*, 1279*w*, 1078*s*, 1015*m*, 963*m*, 930*w*, 848*w*, 816*m*, 800*m*, 740*m*, 624*s*, 463*w*. FAB-MS: 535 ($[M–ClO_4]^+$).

{1,4,8-Trimethyl-11-[4-(methylthio)benzyl]-1,4,8,11-tetraazacyclotetradecane}nickel(II) Diperchlorate: Yield 96%. IR: 3421*m*, 2956*m*, 2017*w*, 1636*m*, 1417*m*, 1090*s*, 962*m*, 802*w*, 759*m*, 740*m*, 624*s*, 463*w*. FAB-MS: 535 ($[M - ClO_4]^+$). Anal. calc. for $C_{21}H_{38}Cl_2N_4NiO_8S$ (636.22): C 39.65, H 6.02, Cl 11.14, N 8.81, Ni 9.22, S 5.04; found: C 39.87, H 5.98, Cl 11.06, N 8.85, Ni 8.94, S 5.25.

{1-(2-Methoxybenzyl)-4,8,11-trimethyl-1,4,8,11-tetraazacyclotetradecane}nickel(II) Diperchlorate: Yield 83%. IR: 3444*m*, 2936*w*, 2008*w*, 1601*w*, 1495*m*, 1468*m*, 1286*w*, 1250*m*, 1091*s*, 1028*m*, 964*w*, 810*w*, 624*s*. FAB-MS: 519 ($[M - ClO_4]^+$).

{1-(4-Methoxybenzyl)-4,8,11-trimethyl-1,4,8,11-tetraazacyclotetradecane}nickel(II) Diperchlorate: Yield 86%. IR: 3423*m*, 2926*w*, 2014*w*, 1610*m*, 1517*m*, 1474*m*, 1253*m*, 1091*s*, 738*w*, 625*m*. FAB-MS: 519 ($[M - ClO_4]^+$).

Cyclic Voltammetry. Voltammetric experiments were performed with a three-electrode cell composed of a saturated calomel reference electrode, a Pt-foil counter electrode and either a static Hg drop electrode of 0.015 cm^2 drop area (*Laboratorni Pristroje*), used in the hanging drop mode (HMDE), or a glassy C electrode (BAS) with a surface area of 0.07 cm^2. Voltammograms were recorded with an *EG & G PARC* model *273* potentiostat controlled *via* ECHEM software on a *PC 486* computer. The COOL algorithm (PAR software) was used to fit the experimental curves to a reversible one-electron process for the electrode reaction at the metal centre. MeCN solns. of the compounds (1 or 2 mM) were prepared daily, and tetrapropylammonium tetrafluoroborate (0.1M in CH_3CN) was used as supporting electrolyte. All electrochemical experiments were done at 25°, using variable scan rates, in solns. deaerated by passing Ar.

Reduction of the Complexes and Detection of Methane. The reactions were carried out with solid Na-amalgam (0.2–2.5 mass-% Na) as reducing agent and dry DMF as solvent. The suspension of Na/Hg in DMF was stirred under N_2 during 15 min, then the complex (1 mM) was added, and at different time intervals, 50-µl probes were taken from the gas phase (250-µl gas-tight syringe (*Hamilton*)) and injected in the gas chromatograph (*Carlo Erba, Fisons 8000*, FID detector), equipped with a *Varian* column (molecular sieve 5 Å, *45/60 SST*). The amount of methane was determined using a calibration curve obtained by injecting known amounts of pure methane (*Carbagas* > 99.5%).

X-Ray Diffraction Measurements. The crystal data and parameters of the data collection for the Ni^{2+} complexes with **1** and **2** are given in *Table 1*. Unit-cell parameters were determined by accurate centering of 25 independent strong reflections by the least-squares method. Three standard reflections monitored every 2 h during data collection showed no significant variation of the intensity. The raw data set was corrected for polarization

Table 1. *Crystal Data and Parameter of Data Collection for the Ni^{2+} Complex with* **1** *and* **2**

	1	**2**
Formula	$(C_{21}H_{38}N_4NiS)(ClO_4)_2$	$(C_{21}H_{38}N_4NiS)(ClO_4)_2$
Mol. wt.	636.22	636.22
Crystal system	triclinic	orthorhombic
Space group	$P\bar{1}$	*Pbca*
a [Å]	9.478(1)	12.658(1)
b [Å]	12.036(1)	18.114(2)
c [Å]	12.515(1)	24.785(2)
α [deg]	82.373(8)	90
β [deg]	78.915(7)	90
γ [deg]	77.999(6)	90
Z	2	8
Volume [Å^3]	1364.0(2)	5683.2(7)
Density [gcm^{-3}]	1.549	1.487
μ [cm^{-1}]	40.09	38.49
F(000)	668	2672
Crystal size [mm]	0.20 × 0.25 × 0.35	0.10 × 0.42 × 0.45
Temperature [K]	293	293
θ_{max} [°]	77.5	77.5
Radiation	CuK_α (λ = 1.54178 Å)	CuK_α (λ = 1.54178 Å)
Scan type	$\omega/2\theta$	$\omega/2\theta$
No. of measured refl.	6002	6364
No. of indep. refl.	5254	5794
No. of refl. in ref.	4212	3629
No. of variables	408	427
Final *R* value [%]	6.06	6.06
Final R_w value [%]	6.93	7.53
Weighting scheme	weight·$[1-(\Delta(F)/6\sigma F)^2]^2$	weight·$[1-(\Delta(F)/6\sigma F)^2]^2$

effects and X-ray diffraction absorption. The structure was solved by the direct method [12]. Anisotropic least-squares refinements were carried out on all non-H-atoms, using the program CRYSTALS [13]. The two ClO_4^- ions are disordered. They have been refined using two split positions per atom keeping the sum of their occupancy equal to 1. H-Atoms are in calculated positions with C–H distances of 0.96 Å and fixed isotropic thermal parameters. Scattering factors are taken from the 'International Tables for Crystallography' [14].

Result and Discussions. – The synthesis of the monofunctionalized ligands is simple, since there is only one secondary amino group in **5** which can be alkylated. We introduced

Table 2. *Absorption Spectra* (λ in nm and ε in M^{-1} cm^{-1}) *of the Ni^{2+} Complexes with Ligands* **1–4** *in Different Solvents*[a])

	1	**2**	**3**	**4**
H_2O	652 (sh)	648 (sh)	654 (sh)	648 (sh)
	539 (58)	538 (64)	533 (75)	538 (119)
	380 (sh)	393 (47)	394 (65)	395 (60)
MeCN	610 (27)	614 (25)	614 (32)	614 (35)
	381 (92)	382 (86)	382 (106)	383 (121)
DMF	672 (22)	672 (24)	674 (33)	678 (38)
	543 (19)	–	500 (sh)	530 (sh)
	402 (78)	403 (82)	402 (113)	404 (126)

[a]) sh = Shoulder.

an *ortho*- or a *para*-substituted benzylic side chain in order to control the structure and the configuration in the complexes formed by these ligands.

The absorption spectra of the Ni^{2+} complexes in different solvents are given in *Table 2*. In H_2O and DMF, three more or less well pronounced bands can be observed, indicating that as for the tmc complexes [15], two species are present: a square-planar one absorbing in the region 530–540 nm, and a pentacoordinated one with two bands at 380–400 and 670 nm. In MeCN, only the pentacoordinated species is present, probably because MeCN can easily coordinate to the axial position of the Ni^{2+}. The observation that the spectra of the different complexes are very similar to each other excludes the possibility that the MeS or the MeO donor group is coordinated to the metal ion, since this would only be possible for the *ortho*- but not for the *para*-substituted derivative.

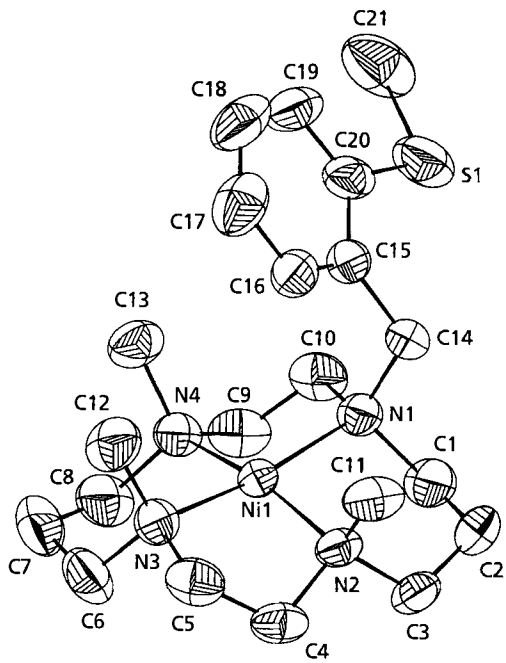

Fig. 1. *ORTEP Plot of the Ni^{2+} complex with* **1**

Table 3. *Selected Bond Lenghts* [Å] *and Angles* [deg] *in the Structure of the Ni^{2+} Complexes with* **1** *and* **2**

	1	**2**		**1**	**2**
Ni(1)–N(1)	2.021(3)	2.002(3)	N(1)–Ni(1)–N(2)	87.2(1)	94.7(2)
Ni(1)–N(2)	1.981(3)	1.982(3)	N(1)–Ni(1)–N(3)	171.2(1)	170.2(2)
Ni(1)–N(3)	1.989(3)	1.989(4)	N(1)–Ni(1)–N(4)	94.5(1)	86.7(1)
Ni(1)–N(4)	1.992(3)	1.973(3)	N(2)–Ni(1)–N(3)	93.7(1)	86.2(2)
Ni(1)–S(1)	5.577(1)	7.070(1)	N(2)–Ni(1)–N(4)	166.4(1)	163.1(1)
S(1)–C(21)	1.793(7)	1.762(7)	N(3)–Ni(1)–N(4)	86.7(1)	95.3(2)

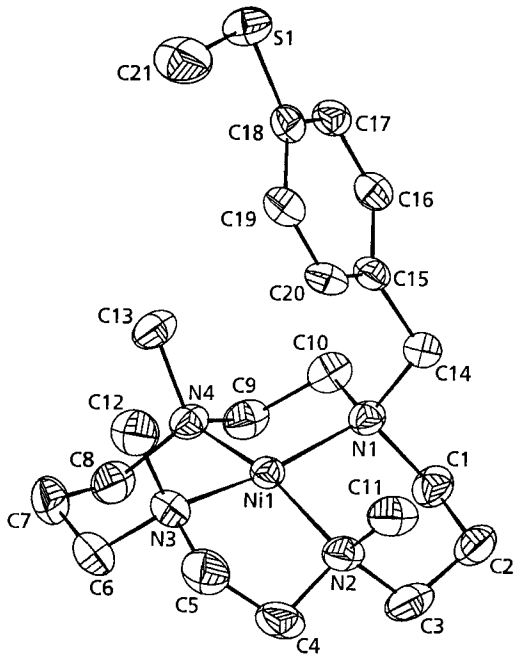

Fig. 2. *ORTEP Plot of the* Ni^{2+} *complex with* **2**

The X-ray structures of the Ni^{2+} complexes with **1** and **2** are shown in *Figs. 1* and *2*, respectively. In both cases, the Ni^{2+} ion is coordinated by the four N-atoms of the macrocycle in a tetrahedrally distorted square-planar arrangement. The deviations of the N-atoms from the best plane are ±0.19 and ±0.23 Å for the complexes with **1** and **2**, respectively, whereas the central ion is virtually in this plane (0.04 and 0.06 Å for the complexes with **1** and **2**, resp.). Both structures closely resemble those observed for other tetra-*N*-substituted 1,4,8,11-tetraazacyclotetradecane complexes [16], the macrocycle being in the *trans-I* configuration. Ni–N Bond lengths are in the normal range (*Table 3*) and the Ni(1)–S(1) distance is such (5.58 and 7.07 Å for the complex with **1** and **2**, resp.) that in both cases no axial interaction can take place. The angles around the Ni^{2+} ion are distinctly different from the ideal values of 90 and 180° (*Table 3*).

The cyclic voltammetry of the complexes with a methylthio pendant chain exhibit a metal ion centered electrode process at potentials between to −0.73 and −0.80 V, corresponding to the Ni^{II}/Ni^{I} system. The characteristics of the voltammetric peaks c_1 and a_1 for the complexes with **1** and **2**, recorded on GCE and HMDE, are given in *Table 4*. The Ni^{II}/Ni^{I} electrode process fits well to the reversible one-electron transfer scheme similar to that observed for $[Ni(cyclam)]^{2+}$ (cyclam = 1,4,8,11-tetraazacyclotetradecane) [17] or its tetramethylated derivative $[NiTMC]^{2+}$ [7]. Similarly reversible are the Ni^{II}/Ni^{I} processes for the tetraazamacrocyclic complexes with the methoxy pendant chain, proving that addition of a pendant arm does not significantly affect the metal ion centered electrode process (*Table 4*).

Table 4. *Characteristics of the Voltammetric Studies for the Ni^{II}/Ni^{I} System in the Complexes with* **1**–**4** (1 mM; 0.1M $Pr_4N(BF_4)$) *in MeCN*

	Hanging Hg drop electrode (HMDE)				Glassy C electrode (GCE)			
	c_1 [V]	a_1 [V]	$E^{o\prime}$ [V]	$E_{c1}-E_{a1}$ [V]	c_1 [V]	a_1 [V]	$E^{o\prime}$ [V]	$E_{c1}-E_{a1}$ [V]
1	−0.729	−0.648	−0.688	0.081	−0.728	−0.657	−0.686	0.071
2	−0.796	−0.710	−0.753	0.086	−0.796	−0.710	−0.753	0.086
3	−0.775	−0.684	−0.730	0.091	−0.769	−0.692	−0.731	0.077
4	−0.776	−0.668	−0.722	0.108	−0.779	−0.670	−0.725	0.109

When the potential range is extended to more negative values, two additional peaks c_2 and c_3 are observed for the complexes with **1** and **2** containing the methylthio group (*Fig. 3*). They represent ligand-centered reductions. No corresponding anodic signal can be observed indicating that the products of the reduction undergo further chemical reactions. A comparison of the voltammograms recorded for the complexes with a methylthio or a methoxy pendant chain in the same position indicates large differences in the behavior of these compounds (*Fig. 3*). Since cleavage of a thioether can more easily take place than cleavage of an ether, this could be responsible for the appearance of peaks c_2 and c_3. To investigate the products formed in this reaction, the potential scan was initialized at potentials negative to those of the cathodic peaks (*Fig. 4*), and the anodic half-cycle was then recorded for the methylthio derivatives **1** and **2**. The anodic half-cycle peak a_x appears at 0.8 V and an additional one at *ca.* 1.3 V. In the case of the *ortho*-derivative, the peak a_x is more clearly developed than in the *para*-derivative. Both the reduction

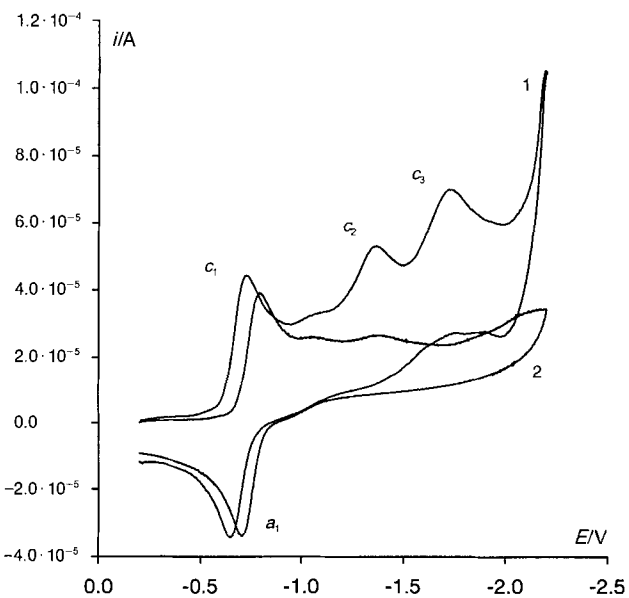

Fig. 3. *Cyclic voltammograms for the Ni^{2+} complexes* (2 mM) *with* **1** (curve 1) *and* **3** (curve 2)

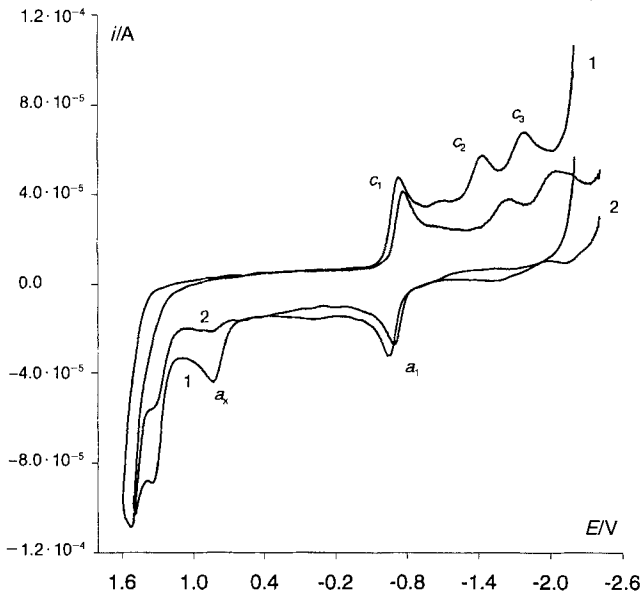

Fig. 4. *Cyclic voltammograms for the* Ni^{2+} *complexes* (2 mM) *with* **1** (curve 1) *and* **2** (curve 2), *the potential scan starting at negative potential*

peaks c_2 and c_3 and the oxidation peak a_x are not present when the methylthio pendant chain is substituted by the methoxy chain.

To find the range of potentials at which the substrate oxidized in peak a_x is produced, the anodic half-cycle was started at different potentials as demonstrated in *Fig. 5*. For the complex with **1**, the peak a_x is not observed when the scan is started at potentials more positive (curve A and B) than peak c_2. However, upon application of potentials C or D, hence negative compared to the peak c_2, the product formed is oxidized leading to the formation of a_x. The anodic signal at more positive potentials than a_x is not connected with ligand-centered reduction and appears to be independent upon the initial potential. It can be ascribed to the oxidation of $[Ni^{II}L]$ diffusing to the electrode surface from the bulk solution. At lower scan rates, a cathodic counterpart of this signal is seen.

In similar studies but using the *ortho*-methoxy derivative (Ni^{2+} complex with **3**), peaks c_2 and c_3 are not developed, and no a_x signal is observed. This confirms that the C–S bond cleavage gives rise to peak a_x, and that the anodic signal may be ascribed to thiolate oxidation. The voltammograms shown in *Fig. 4* indicate that the thiolate is formed most readily when the compound has an *ortho*-methylthio group in the side chain. A poorly developed signal is seen for the corresponding *para*-form and indicates the importance of the position of the methylthio group relative to the Ni^{I} center in the C–S bond cleavage.

Additional measurements were run on a hanging Hg drop electrode. Thiolates are known to promote the oxidation of Hg, whereby poorly-soluble products of this oxidation are deposited on the electrode surface [18]. A Hg electrode should, therefore, be appropriate for detecting bond cleavage and formation of thiolate in the reduction of our

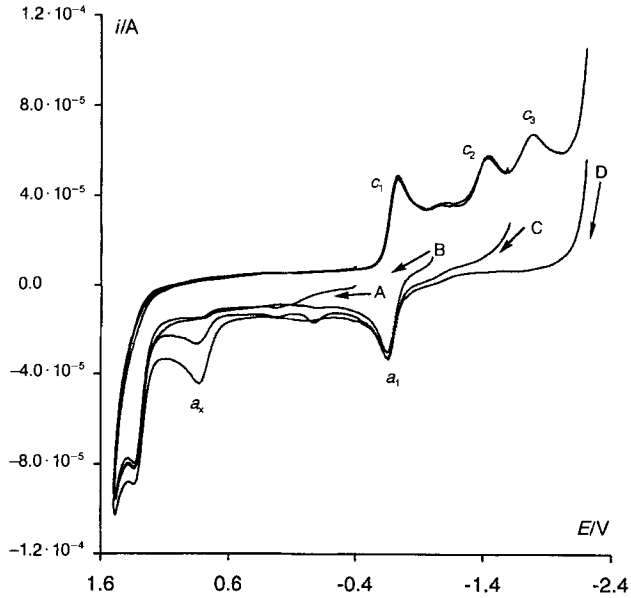

Fig. 5. *Influence of starting potential on the cyclic voltammogram of the* Ni^{2+} *complex with* **1** (2 mM). Initial potentials: −0.2 (A), −1.0 (B), −1.6 (C) and −2.2 V (D).

compounds. On the Hg electrode, the c_1/a_1 system of peaks is also reversible, although additional peaks indicate that the processes studied are complicated by adsorption. The c_2 and c_3 peaks for the complex with **1** are clearly developed at −1.5 and −1.95 V. The c_3 peak has even an anodic counterpart at −1.8 V, which indicates that Hg stabilizes the product against further chemical reactions. When the anodic half-cycle is recorded for the Ni^{2+} complexes of all four compounds starting at −2.5 V, the *ortho*-methylthio compound **1** is immediately recognized by the appearance of a large and narrow peak of the Hg oxidation in the presence of thiolate released upon reduction of the complex. This a_x' signal has its reduction counterpart c_x' corresponding to the reduction of the Hg compound. Much smaller, but still present, is the a_x'/c_x' system for the *para*-methylthio derivative (complex with **2**), while no such peaks are observed for the *ortho*- and *para*-methoxy derivatives (complexes with **3** and **4**, resp.).

Among the compounds studied in this work, the Ni^{2+} complex of **1** is thus the best model for C–S bond cleavage with formation of the corresponding thiol and methane. Since the latter is not electroactive and its formation cannot be proved by electrochemistry, additional experiments were run. Solutions of the Ni^{2+} complexes with **1** and **2** in DMF were treated with Na-amalgam as reducing agent. Rapidly the color changed from blue to yellow-green indicating that, in analogy to the electrochemistry, Ni^{II} was reduced to Ni^{I}. At fixed time intervals, probes from the gas phase over the solution were taken with a gas-tight syringe and injected into a gas chromatograph equipped with a column able to detect methane. Using a calibration curve, the amount of methane could be determined quantitatively. In the case of the Ni^{2+} complex with **2**, no methane was found, whereas for the complex with **1**, methane production was observed. Although the amount

reached after 10 h was relatively small (*ca.* 5%), the difference between the two complexes with an *ortho*- and *para*-methylthio group is significant and perhaps indicates that the close proximity of the Ni^{I} centre to the MeS group, which only occurs for ligand **1**, is important for this process.

This work was supported by the *Bundesamt für Bildung und Wissenschaft* through a *COST-D1* grant, an this is gratefully acknowledged. We also thank the University of Warsaw for supporting the electrochemical work through grant *BST 502*.

REFERENCES

[1] E. Hörmann, P. C. Riesen, M. Neuburger, M. Zehnder, Th. A. Kaden, *Helv. Chim. Acta* **1996,** *79,* 235.
[2] B. Jaun, *Metal Ions Biol. Syst.* **1993,** *29,* 287.
[3] A. Pfaltz, B. Jaun, A. Fässler, A. Eschenmoser, R. Jeanchen, H. H. Giles, G. Diekert, R. K. Thauer, *Helv. Chim. Acta* **1982,** *65,* 828; A. Fässler, A. Kobelt, A. Pfaltz, A. Eschenmoser, C., Bladen, A. R. Battersby, R. K. Thauer, *ibid.* **1985,** *68,* 2287; G. Färber, W. Keller, C. Kratky, B. Jaun, A. Pfaltz, C. Spinner, A. Kobelt, A. Eschenmoser, *ibid.* **1991,** *74,* 697.
[4] M. Zimmer, R. H. Crabtree, *J. Am. Chem. Soc.* **1990,** *112,* 1062; A. Fässler, Ph. D. Thesis, No. 7799, ETH-Zürich, 1985; C. L. Hamilton, R. A. Scott, M. K. Johnson, *J. Biol. Chem.* **1989,** *264,* 11605; G. P. Diakun, B. Piggott, H. J. Tinton, D. Ankel-Fuchs, R. K. Thauer, *Biochem. J.* **1985,** *232,* 281; A. K. Shiemke, J. A. Shelnutt, R. A. Scott, *J. Biol. Chem.* **1989,** *264,* 11236; A. K. Shiemke, W. A. Kaplan, C. L. Hamilton, J. A. Shelnutt, R. A. Scott, *ibid.* **1989,** *264,* 7276.
[5] B. Jaun, *Helv. Chim. Acta* **1990,** *73,* 2209.
[6] B. Jaun, A. Pfaltz, *J. Chem. Soc., Chem. Commun.* **1986,** 1327.
[7] E. K. Barefield, G. M. Freemann, D. G. Van Derveer, *Inorg. Chem.* **1986,** *25,* 552; M. S. Ram, S. Riordan, *J. Am. Chem. Soc.* **1995,** *117,* 2365.
[8] E. K. Barefield, F. Wagner, U. D. Hodges, *Inorg. Chem.* **1976,** *15,* 1370; F. Wagner, E. K. Barefield, *ibid.* **1976,** *15,* 408.
[9] P. Clark, D. Ewing, F. Kerrigan, R. Scrowston, *J. Chem. Soc., Perkin Trans. 1* **1982,** 615.
[10] A. Ullman, C. Willand, W. Koehler, D. Robello, D. Williams, L. Handley, *J. Am. Chem. Soc.* **1990,** *112,* 7083.
[11] A. Shantu, S. Hecht, D. Hoffmann, *J. Org. Chem.* **1981,** *46,* 2394.
[12] A. Altomare, G. Cascarano, G. Giacovazzo, A. Guagliardi, M. C. Burla, G. Polidori, M. Camalli, *J. Appl. Crystallogr.* **1994,** *27,* 435.
[13] D. Watkin, R. Carruthers, P. Betteridge, 'CRYSTALS', Chemical Crystallography Laboratory, Oxford, 1990.
[14] 'International Tables for Crystallography', Kynoch Press, Birmingham, 1974, Vol. IV, Table 2.2B.
[15] M. Micheloni, P. Paoletti, S. Bürki, Th. A. Kaden, *Helv. Chim. Acta* **1982,** *65,* 587.
[16] J. C. Boyens, S. M. Dobson, in 'Stereochemical and Stereophysical Behaviour of Macrocycles', Ed. I. Bernal, Elsevier, Amsterdam, 1987, Vol. 2, p. 1; M. Oberholzer, M. Neuburger, M. Zehnder, Th. A. Kaden, *Helv. Chim. Acta* **1995,** *78,* 505; T. Hiroshi, *J. Chem. Soc., Chem. Commun.* **1983,** 970; N. W. Alcock, A. Benniston, S. J. Grant, H. A. A. Omar, P. Moore, *ibid.* **1991,** 1573.
[17] F. V. Lovecchio, E. S. Gore, D. H. Busch, *J. Am. Chem. Soc.* **1974,** *96,* 3109.
[18] T. M. Florence, *J. Electroanal. Chem.* **1979,** *97,* 219.